Chapter 12

SPATIAL CHARACTERIZATION OF MULTIPLE ANTENNA CHANNELS

Tony S. Pollock, Thushara D. Abhayapala, and Rodney A. Kennedy
Wireless Signal Processing Program, National ICT Australia, and Department of Telecommunications Engineering, RSISE, The Australian National University, Locked Bag 8001, Canberra ACT 2601, Australia.
(tony.pollock, thushara.abhayapala, rodney.kennedy)@nicta.com.au

Abstract In this chapter we present a realistic new model for wireless multiple-input multiple-output (MIMO) channels which is more general than previous models. A novel spatial decomposition of the channel is developed to provide insights into the spatial aspects of multiple antenna communication systems. By exploiting the underlying physics of free-space wave propagation we characterize the fundamental communication modes of a physical aperture and develop an intrinsic capacity which is independent of antenna array geometries and array signal processing. We show there exists a maximum achievable capacity for communication between spatial regions of space, which depends on the size of the regions and the statistics of the scattering environment.

Keywords: multiple antennas, capacity, antenna arrays, MIMO, channel modelling

1. INTRODUCTION

Multiple-Input Multiple-Output (MIMO) communications systems using multi-antenna arrays simultaneously during transmission and reception have generated significant interest in recent years. Theoretical work of [1,2] showed the potential for significant capacity increases in wireless channels via spatial multiplexing with sparse antenna arrays. With these developments comes the need for better understanding of the spatial properties of the wireless communications channel. The spatial properties of multiple antenna channels have significant impact on the capacity of MIMO systems, therefore, a good understanding of these properties

is required for effective design and implementation of wireless MIMO systems.

For randomly fading channels, much of the literature is limited to the idealistic situation of independent and identically distributed (i.i.d.) Gaussian channels, where the channel gains are modelled as independent Gaussian random variables (for example see [1, 2]). The i.i.d. model corresponds to sufficiently spaced antennas such that there is no spatial correlation between antenna elements at the transmit and receive arrays, along with significant scattering between arrays. However, in practice, realistic scattering environments and limited antenna separation leads to channels which exhibit correlated fades.

For correlated fading, MIMO channel modelling can be approached via field measurements [3–6], and deterministic physical models such as ray tracing [7, 8], where the significant characteristics of the channel are obtained and incorporated into the model. Such methods give an accurate characterization of the channel, however, they are computationally expensive and provide results for specific scenarios only. Finally, a statistical model can be postulated which attempts to capture the physical channel characteristics based on the basic principles of radio propagation [9–12]. These scattering models can often be used as simple analysis tools which illustrate the essential characteristics of the MIMO channel, provided the constructed scattering environment is reasonable.

With the notable exception of [10] and [12], the statistical models mentioned above have poor physical significance. In particular, the separate effects of the scatterers and the antenna correlation are not accounted for. As outlined in [10], the models assume that only the spatial fading correlation is responsible for the rank structure of the MIMO channel. In practice, however, high rank MIMO channels correspond not only to the low fading correlation, but also to the structure of scattering in the propagation environment.

The models presented in [10, 12] allow for insight into the effects of spatial correlation and scattering, however, they are unfortunately limited to particular array geometries and model the scattering environment using a discrete representation. Therefore, although offering considerable insight into the scattering characteristics of the channel they are restricted spatially, in the sense that the antenna geometry is restricted to a particular array configuration and discrete scattering environments.

In contrast to previous models, the contribution of this chapter is a spatial channel model which includes the physical parameters of arbitrary antenna configurations and a tractable parameterization of the complex scattering environment. We approach the MIMO channel modelling problem from a physical wave field perspective. By using the

underlying physics of free-space wave propagation we explore the fundamental properties of the channel due to constraints imposed by the basic laws governing wave field behavior. Furthermore, we show that there exists a maximum achievable capacity for communication between spatial regions of space, which depends on the size of the regions and the statistics of the scattering environment. This bound on capacity gives the optimal MIMO capacity and thus provides a benchmark for future array and space-time coding developments.

2. CHANNEL MODEL

Consider the 2D MIMO system shown in Fig. 12-1, where the transmitter consists of n_{T} transmit antennas located within a circular aperture of radius r_{T}. Similarly, at the receiver, there are n_{R} antennas within a circular aperture of radius r_{R}. Denote the n_{T} transmit antenna positions by $\boldsymbol{x}_t = (\|\boldsymbol{x}_t\|, \theta_t)$, $t = 1, 2, \ldots, n_{\mathrm{T}}$, in polar coordinates, relative to the origin of the transmit aperture, and the n_{R} receive antenna positions by $\boldsymbol{y}_r = (\|\boldsymbol{y}_r\|, \varphi_r)$, $r = 1, 2, \ldots, n_{\mathrm{R}}$, relative to the origin of the receive aperture. Note that all transmit and receive antennas are constrained to within the transmit and receive apertures respectively, that is, $\|\boldsymbol{x}_t\| \leq r_{\mathrm{T}}, \forall t$, and $\|\boldsymbol{y}_r\| \leq r_{\mathrm{R}}, \forall r$. It is also assumed that the scatterers are distributed in the farfield from all transmit and receive antennas, therefore, define circular scatterer free regions of radius $r_{\mathrm{TS}} > r_{\mathrm{T}}$, and $r_{\mathrm{RS}} > r_{\mathrm{R}}$, such that any scatterers are in the farfield to any antenna within the transmit and receive apertures, respectively.

Finally, the random scattering environment is defined by the effective random complex scattering gain $g(\phi, \psi)$ for a signal leaving from the transmit aperture at an angle ϕ, and entering the receive aperture at an angle ψ, via any number of paths through the scattering environment.

Consider the narrowband transmission of n_{T} baseband signals, $\{x_t\}$, $t = 1, \ldots, n_{\mathrm{T}}$, over a single signalling interval from the n_{T} transmit antennas located within the transmit aperture. From Fig. 12-1 the noiseless signal at $\boldsymbol{y}_r$ is given by

$$z_r = \sum_{t=1}^{n_{\mathrm{T}}} x_t \iint_{\mathbb{S}^1} g(\phi, \psi)\, e^{ik\|\boldsymbol{x}_t\| \cos(\theta_t - \phi)}\, e^{-ik\|\boldsymbol{y}_r\| \cos(\varphi_r - \psi)}\, d\phi d\psi. \quad (12.1)$$

where $\mathbb{S}^1$ denotes the unit circle.

Denote $\boldsymbol{x} = [x_1, x_2, \ldots, x_{n_{\mathrm{T}}}]'$ as the column vector of the transmitted signals, and $\boldsymbol{n} = [n_1, n_2, \ldots, n_{n_{\mathrm{R}}}]'$, as the noise vector where n_r is the independent additive white Gaussian noise (AWGN) with variance $N_0 \in \mathcal{N}(0, 1)$ at the r-th receive antenna, then the vector of received signals

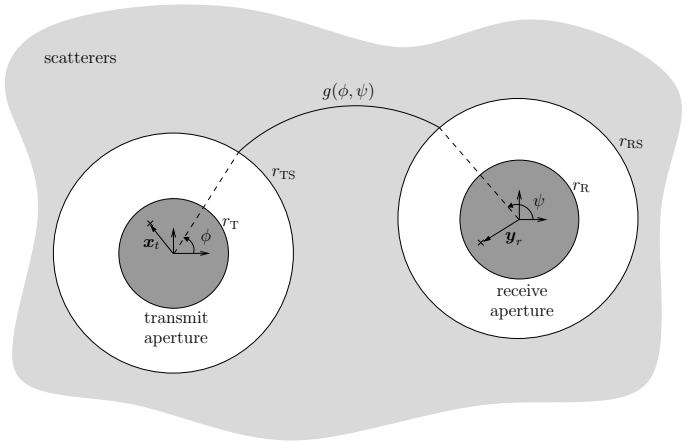

Figure 12-1. Scattering model for a 2D flat fading narrowband MIMO system. r_{T} and r_{R} are the radii of circular apertures which contain the transmit and receive antenna arrays, respectively. The radii r_{TS} and r_{RS} describe scatterer free circular regions surrounding the transmit and receive apertures, assumed large enough that any scatterer is farfield to all antennas. The scattering environment is described by $g(\phi,\psi)$ which gives the effective random complex gain for signals departing the transmit aperture from angle ϕ and arriving at the receive aperture from angle ψ, via any number of scattering paths.

$\boldsymbol{y} = [y_1, y_2, \ldots, y_{n_{\mathrm{R}}}]'$ is given by

$$\boldsymbol{y} = \boldsymbol{H}\boldsymbol{x} + \boldsymbol{n}, \tag{12.2}$$

where $\boldsymbol{H}$ is the complex random channel matrix with r,t-th element

$$\boldsymbol{H}|_{r,t} = \iint_{\mathbb{S}^1} g(\phi,\psi) e^{ik\|\boldsymbol{x}_t\|\cos(\theta_t-\phi)}\, e^{-ik\|\boldsymbol{y}_r\|\cos(\varphi_r-\psi)}\, d\phi d\psi, \tag{12.3}$$

representing the channel gain between the t-th transmit antennna and the r-th receive antenna.

2.1 Channel Matrix Decomposition

Consider the modal expansion[1] of the plane wave [13]

$$e^{ik\|\boldsymbol{x}\|\cos(\theta_x-\phi)} = \sum_{n=-\infty}^{\infty} i^n J_n(k\|\boldsymbol{x}\|) e^{-in(\theta_x-\phi)}, \tag{12.4}$$

[1]Each mode, indexed by n, corresponds to a different solution of the governing electromagnetic equations (Maxwell's equations) for the given boundary conditions.

for vector $\boldsymbol{x} = (\|\boldsymbol{x}\|, \theta_x)$, and $J_n(\cdot)$ are the Bessel functions of the first kind.

Bessel functions $J_n(z)$, $|n| > 0$ exhibit spatially high pass behavior, that is, for fixed order n, $J_n(z)$ starts small and becomes significant for arguments $z \approx \mathcal{O}(n)$. Therefore, for a fixed argument z, the Bessel function $J_n(z) \approx 0$ for all but a finite set of low order modes $n \leq N$, hence (12.4) is well approximated by the finite sum

$$e^{ik\|\boldsymbol{x}\|\cos(\theta_x - \phi)} \simeq \sum_{n=-N}^{N} \overline{\mathcal{J}_n(\boldsymbol{x})} e^{in\phi}, \tag{12.5}$$

where $\overline{\mathcal{J}_n(\boldsymbol{x})}$ is the complex conjugate of function $\mathcal{J}_n(\boldsymbol{x})$, defined as the *spatial-to-mode* function

$$\mathcal{J}_n(\boldsymbol{x}) \triangleq J_n(k\|\boldsymbol{x}\|) e^{in(\phi_x - \pi/2)}, \tag{12.6}$$

which maps the sampling point $\boldsymbol{x}$ to the nth mode of the expansion (12.4). In [14] it was shown that $J_n(z) \approx 0$ for $n > \lceil ze/2 \rceil$, with $\lceil \cdot \rceil$ the ceiling operator. Therefore, we can define

$$N_{\mathrm{T}} \triangleq \lceil \pi e r_{\mathrm{T}} / \lambda \rceil, \tag{12.7}$$

$$N_{\mathrm{R}} \triangleq \lceil \pi e r_{\mathrm{R}} / \lambda \rceil, \tag{12.8}$$

such that the truncated expansions

$$e^{ik\|\boldsymbol{x}_t\|\cos(\theta_t - \phi)} \simeq \sum_{n=-N_{\mathrm{T}}}^{N_{\mathrm{T}}} \overline{\mathcal{J}_n(\boldsymbol{x}_t)} e^{in\phi}, \tag{12.9}$$

$$e^{-ik\|\boldsymbol{y}_r\|\cos(\varphi_r - \psi)} \simeq \sum_{m=-N_{\mathrm{R}}}^{N_{\mathrm{R}}} \mathcal{J}_m(\boldsymbol{y}_r) e^{-in\psi}, \tag{12.10}$$

hold for every antenna within the transmit and receive apertures of radius r_{T} and r_{R}, respectively.

Substitution of (12.9) and (12.10) into (12.3), gives the closed-form expression for the channel gain between the t-th transmit antenna and r-th receive antenna as

$$\boldsymbol{H}|_{r,t} = \sum_{n=-N_{\mathrm{T}}}^{N_{\mathrm{T}}} \sum_{m=-N_{\mathrm{R}}}^{N_{\mathrm{R}}} \overline{\mathcal{J}_n(\boldsymbol{x}_t)} \mathcal{J}_m(\boldsymbol{y}_r) \iint_{\mathbb{S}^1} g(\phi, \psi) e^{in\phi} e^{-im\psi} d\phi d\psi. \tag{12.11}$$

From (12.11) the channel matrix $\boldsymbol{H}$ can be decomposed into a product of three matrices, which correspond to the three spatial regions of signal

propagation,

$$\boldsymbol{H} = \boldsymbol{J}_{\mathrm{R}} \boldsymbol{H}_{\mathrm{S}} \boldsymbol{J}_{\mathrm{T}}^{\dagger}, \tag{12.12}$$

where $\boldsymbol{J}_{\mathrm{T}}$ is the $n_{\mathrm{T}} \times (2N_{\mathrm{T}} + 1)$ *transmit aperture sampling* matrix,

$$\boldsymbol{J}_{\mathrm{T}} = \begin{bmatrix} \mathcal{J}_{-N_{\mathrm{T}}}(\boldsymbol{x}_1) & \cdots & \mathcal{J}_{N_{\mathrm{T}}}(\boldsymbol{x}_1) \\ \mathcal{J}_{-N_{\mathrm{T}}}(\boldsymbol{x}_2) & \cdots & \mathcal{J}_{N_{\mathrm{T}}}(\boldsymbol{x}_2) \\ \vdots & \ddots & \vdots \\ \mathcal{J}_{-N_{\mathrm{T}}}(\boldsymbol{x}_{n_{\mathrm{T}}}) & \cdots & \mathcal{J}_{N_{\mathrm{T}}}(\boldsymbol{x}_{n_{\mathrm{T}}}) \end{bmatrix}, \tag{12.13}$$

which describes the sampling of the transmit aperture, $\boldsymbol{J}_{\mathrm{R}}$ is the $n_{\mathrm{R}} \times (2N_{\mathrm{R}} + 1)$ *receive aperture sampling* matrix,

$$\boldsymbol{J}_{\mathrm{R}} = \begin{bmatrix} \mathcal{J}_{-N_{\mathrm{R}}}(\boldsymbol{y}_1) & \cdots & \mathcal{J}_{N_{\mathrm{R}}}(\boldsymbol{y}_1) \\ \mathcal{J}_{-N_{\mathrm{R}}}(\boldsymbol{y}_2) & \cdots & \mathcal{J}_{N_{\mathrm{R}}}(\boldsymbol{y}_2) \\ \vdots & \ddots & \vdots \\ \mathcal{J}_{-N_{\mathrm{R}}}(\boldsymbol{y}_{n_{\mathrm{R}}}) & \cdots & \mathcal{J}_{N_{\mathrm{R}}}(\boldsymbol{y}_{n_{\mathrm{R}}}) \end{bmatrix}, \tag{12.14}$$

which describes the sampling of the receive aperture, and $\boldsymbol{H}_{\mathrm{S}}$ is a $(2N_{\mathrm{R}}+1) \times (2N_{\mathrm{T}} + 1)$ *scattering environment* matrix, with p, q-th element

$$\boldsymbol{H}_{\mathrm{S}}|_{p,q} = \iint_{\mathbb{S}^1} g(\phi, \psi) e^{i(q - N_{\mathrm{T}} - 1)\phi} e^{-i(p - N_{\mathrm{R}} - 1)\psi} d\phi d\psi, \tag{12.15}$$

representing the complex gain between the $(q - N_{\mathrm{T}} - 1)$-th mode of the transmit aperture and the $(p - N_{\mathrm{R}} - 1)$-th mode of the receive aperture[2].

The channel matrix decomposition (12.12) separates the channel into three distinct regions of signal propagation: free space transmitter region, scattering region, and free space receiver region, as shown in Fig. 12-1. The transmit aperture and receive aperture sampling matrices, $\boldsymbol{J}_{\mathrm{T}}$ and $\boldsymbol{J}_{\mathrm{R}}$, describe the mapping of the transmitted signals to the modes of the system, and the modes to received signals, given the respective positions of the antennas, and are constant for fixed antenna locations within the spatial apertures. Conversely, for a random scattering environment the scattering channel matrix $\boldsymbol{H}_{\mathrm{S}}$ will have random elements.

3. MODE-TO-MODE COMMUNICATION

It is well known that the rank of the channel matrix $\boldsymbol{H}$ gives the effective number of independent parallel channels between the transmit and receive antenna arrays, and thus determines the capacity of

[2]It is important to note the distinction between the *mode-to-mode* gains due to the scattering environment described by $\boldsymbol{H}_{\mathrm{S}}$, and the *antenna-to-antenna* channel gains described by $\boldsymbol{H}$.

the system. For the decomposition (12.12) the rank of $\boldsymbol{H}$ is given by $\min\{\text{rank}(\boldsymbol{J_T}), \text{rank}(\boldsymbol{J_R}), \text{rank}(\boldsymbol{H}_\text{S})\}$, which for a large number of antennas and finite regions, becomes $\min\{2N_\text{T}+1, 2N_\text{R}+1, \text{rank}(\boldsymbol{H}_\text{S})\}$. Therefore we see that the number of available modes for the transmit and receive apertures, determined by the size of the apertures, and any possible modal correlation or key-hole effects [15] (rank 1 $\boldsymbol{H}_\text{S}$) limit the capacity of the system, regardless of how many antennas are packed into the apertures.

Assume $n_\text{T} = 2N_\text{T}+1$ and $n_\text{R} = 2N_\text{R}+1$ antennas are optimally placed (perfect spatial-to-mode coupling) within the transmit and receive regions of radius r_T and r_R, respectively, with total transmit power P_T. In this situation $\boldsymbol{J}_\text{T}\boldsymbol{J}_\text{T}^\dagger = \boldsymbol{I}$ and $\boldsymbol{J}_\text{R}^\dagger\boldsymbol{J}_\text{R} = \boldsymbol{I}$, hence the transmit and receive aperture sampling matrices are unitary and $\boldsymbol{H}_\text{S}$ is then unitarily equivalent to $\boldsymbol{H}$. The instantaneous channel capacity with no channel state information at the transmitter and full channel knowledge at the receiver [2] is then given by

$$C = \log\left|\boldsymbol{I}_{2N_\text{R}+1} + \frac{\eta}{2N_\text{T}+1}\boldsymbol{H}_\text{S}\boldsymbol{H}_\text{S}^\dagger\right|, \tag{12.16}$$

where $\eta = P_\text{T}/N_0$ is the average SNR at any point within the receive aperture.

The ergodic capacity of uniform linear (ULA) and uniform circular (UCA) arrays are shown in Fig. 12-2 for an increasing number of antennas constrained within transmit and receive apertures of radius 0.8λ, i.e. the physical size of the array remains fixed as the number of antennas is increased. Here we can see that by spatially constraining the antenna arrays the capacity growth saturates and, unlike the i.i.d. case, provides no further capacity improvement with increasing numbers of antennas. The mode-to-mode capacity (12.16) represents the intrinsic capacity for communication between two spatial apertures, giving the maximum capacity for all possible array configurations and array signal processing. We can see from (12.7) and (12.8) that the intrinsic capacity is limited by the size of the regions containing the antenna arrays (number of available modes), and the statistics of the scattering channel matrix (modal correlation).

Fig. 12-3 shows the radiation pattern of the first 6 modes of the circular and spherical apertures[3]. Each mode has a unique radiation pattern, therefore, mode-to-mode communication can be considered as a pattern diversity scheme, where the signals obtained by different modes may

[3]For extension of the model to the 3D spatial environment see [17].

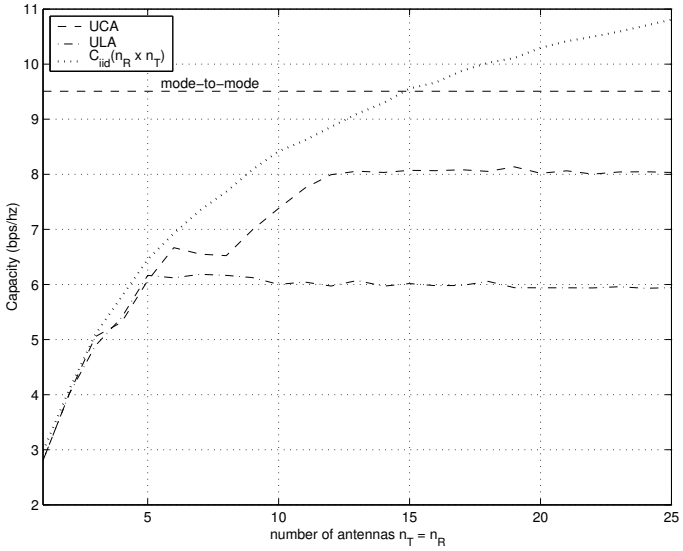

Figure 12-2. Ergodic capacity for increasing number of antennas of uniform linear (ULA) and uniform circular (UCA) arrays constrained within spatial regions of radius 0.8λ and isotropic scattering. The mode-to-mode capacity gives the maximum achievable capacity between the two apertures.

be combined to yield a diversity gain. However, the level of diversity achieved depends on the correlation between the modes, which strongly depends on the scattering environment as shown in the following section.

4. PROPERTIES AND STATISTICS OF SCATTERING CHANNEL MATRIX $\boldsymbol{H}_{\mathbf{S}}$

As the scattering gain function $g(\phi, \psi)$ is periodic with ϕ and ψ it can be expressed using a Fourier expansion. For this 2D model with circular apertures a natural choice of basis functions are the orthogonal circular harmonics $e^{in\phi}$ which form a complete orthogonal function basis set on the unit circle[4], thus express

$$g(\phi, \psi) = \frac{1}{4\pi^2} \sum_{n=-\infty}^{\infty} \sum_{m=-\infty}^{\infty} \beta_m^n e^{-in\phi} e^{im\psi}, \tag{12.17}$$

[4]with respect to the natural inner product $\langle f, g \rangle = \int_0^{2\pi} f(\phi)\overline{g(\phi)}d\phi$

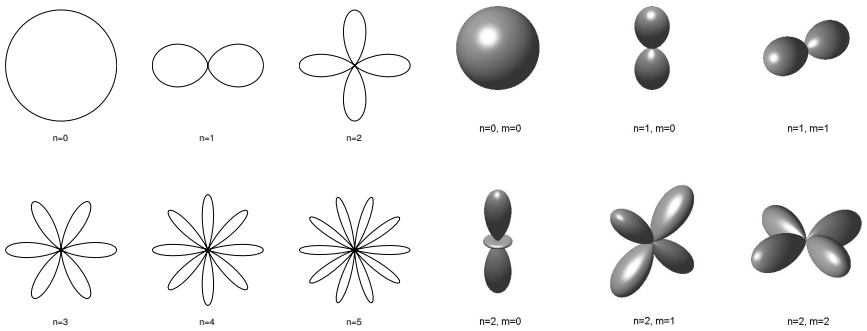

Figure 12-3. Radiation patterns of the first 6 modes of a (a) circular and (b) spherical aperture.

with coefficients

$$\beta_m^n = \iint_{\mathbb{S}^1} g(\phi,\psi) e^{in\phi} e^{-im\psi} d\phi d\psi. \tag{12.18}$$

Therefore, letting $n = q - N_{\mathrm{T}} - 1$, and $m = p - N_{\mathrm{R}} - 1$ denote the transmitter mode and receiver mode index, respectively, the scattering environment matrix coefficients are given by

$$\boldsymbol{H}_{\mathrm{S}}|_{p,q} = \beta_{p-N_{\mathrm{R}}-1}^{q-N_{\mathrm{T}}-1} = \beta_m^n. \tag{12.19}$$

Thus the random scattering environment can be parameterized by the complex random coefficients β_m^n, $n = -N_{\mathrm{T}}, \ldots, N_{\mathrm{T}}$, $m = -N_{\mathrm{R}}, \ldots, N_{\mathrm{R}}$, which gives the scattering gain between the n-th transmit mode and the m-th receive mode, and $\boldsymbol{H}_{\mathrm{S}}$ becomes

$$\boldsymbol{H}_{\mathrm{S}} = \begin{bmatrix} \beta_{-N_{\mathrm{R}}}^{-N_{\mathrm{T}}} & \cdots & \beta_{-N_{\mathrm{R}}}^{N_{\mathrm{T}}} \\ \beta_{-N_{\mathrm{R}}+1}^{-N_{\mathrm{T}}} & \cdots & \beta_{-N_{\mathrm{R}}+1}^{N_{\mathrm{T}}} \\ \vdots & \ddots & \vdots \\ \beta_{N_{\mathrm{R}}}^{-N_{\mathrm{T}}} & \cdots & \beta_{N_{\mathrm{R}}}^{N_{\mathrm{T}}} \end{bmatrix}. \tag{12.20}$$

Assuming a zero-mean uncorrelated scattering environment (Rayleigh), the scattering channel is characterized by the second-order statistics of the scattering gain function $g(\phi,\psi)$, given by,

$$E\left\{ g(\phi,\psi)\overline{g(\phi',\psi')} \right\} = G(\phi,\psi)\delta(\phi-\phi')\delta(\psi-\psi'), \tag{12.21}$$

where $\delta(\cdot)$ is the Kronecker delta function, and $G(\phi,\psi) = E\left\{|g(\phi,\psi)|^2\right\}$ is the 2D power spectral density (PSD) of the modal correlation function,

$$\begin{aligned}\gamma_{n-n',m-m'} &\triangleq E\left\{\beta_m^n \overline{\beta_{m'}^{n'}}\right\} \\ &= \iint_{\mathbb{S}^1} G(\phi,\psi) e^{i(n-n')\phi} e^{-i(m-m')\psi} d\phi d\psi, \end{aligned} \tag{12.22}$$

and represents the scattering channel power over departure and arrival angles ϕ and ψ, normalized such that the total scattering channel power

$$\sigma^2_{\boldsymbol{H}_{\mathrm{S}}} = \iint_{\mathbb{S}^1} G(\phi,\psi) d\phi d\psi = 1. \tag{12.23}$$

For the special case of uniform PSD, $G(\phi,\psi) = 1/4\pi^2$, the modal correlation becomes

$$\gamma_{n-n',m-m'} = \gamma_{0,0}\delta_{n-n'}\delta_{m-m'}, \tag{12.24}$$

corresponding to the i.i.d. $\{\beta_n^m\}$ case.

4.1 Modal Correlation in General Scattering Environments

Define $\mathcal{P}(\psi)$ as the average power density of the scatterers surrounding the receiver, given by the marginalized PSD

$$\mathcal{P}(\psi) \triangleq \int_{\mathbb{S}^1} G(\phi,\psi)\, d\phi, \tag{12.25}$$

then, from (12.22) we see the modal correlation between the m and m' communication modes at the receiver is given by

$$\gamma_{m-m'} = \int_{\mathbb{S}^1} \mathcal{P}(\psi) e^{-i(m-m')\psi} d\psi, \tag{12.26}$$

which gives the modal correlation for all common power distributions $\mathcal{P}(\psi)$: von-Mises, gaussian, truncated gaussian, uniform, piecewise constant, polynomial, Laplacian, Fourier series expansion, etc. Similarly, defining $\mathcal{P}(\phi)$ as the power density of the scatterers surrounding the transmitter, we have the modal correlation at the transmitter

$$\gamma_{n-n'} = \int_{\mathbb{S}^1} \mathcal{P}(\phi) e^{i(n-n')\phi} d\phi. \tag{12.27}$$

As shown in [18] there is very little variation in the correlation due to the various non-isotropic distributions mentioned above, therefore

without loss of generality, we restrict our attention to the case of energy arriving uniformly over limited angular spread Δ around mean ψ_0, i.e., $(\psi_0 - \Delta, \psi_0 + \Delta)$. In this case the modal correlation is given by

$$\gamma_{m-m'} = \text{sinc}((m - m')\Delta)e^{-i(m-m')\psi_0}, \tag{12.28}$$

which is shown in Fig. 12-4 for various modes and angular spread. As one would expect, for increasing angular spread we see a decrease in modal correlation, with more rapid reduction for well separated mode orders, e.g. large $|m - m'|$. For the special case of a uniform isotropic scattering environment, $\Delta = \pi$, we have zero correlation between all modes, e.g., $\gamma_{m-m'} = \delta_{m-m'}$.

Fig. 12-5 shows the impact of modal correlation on the ergodic mode-to-mode capacity for increasing angular spread at the transmitter and isotropic scattering at the receiver[5] for 10dB SNR. We consider transmit and receive apertures of radius 0.8λ, corresponding to $2\lceil \pi e 0.8 \rceil + 1 = 15$ modes at each aperture. For comparison, the capacity for a 15 antenna ULA and UCA, contained within the same aperture size is presented. Also shown is the 15×15 antenna i.i.d. case, corresponding to the rich scattering environment with no restrictions on the antenna placement, i.e., $r_{\text{T}}, r_{\text{R}} \to \infty$.

The mode-to-mode capacity is the maximum achievable capacity between the two apertures, and represents the upper bound on capacity for any antenna array geometry or multi-mode antennas constrained within those apertures. All four cases show no capacity growth for angular spread greater than approximately 60°, which corresponds to low modal correlations ($\ll 0.5$) for the majority of modes, as seen in Fig. 12-4.

5. DISCUSSION

In this chapter we have presented a novel multiple antenna channel model which includes the spatial aspects of a MIMO system not previously considered. The spatial channel model developed includes the physical parameters of arbitrary antenna configurations (number of antenna and their location) and a tractable parameterization of the complex scattering environment.

Using the model we have developed a new upper bound on the capacity for communication between regions in space. Using the underlying physics of free space wave propagation we have shown that there is a

[5]This models a typical mobile communication scenario, where the receiver is usually surrounded by scatterers, and the base station is mounted high above the scattering environment.

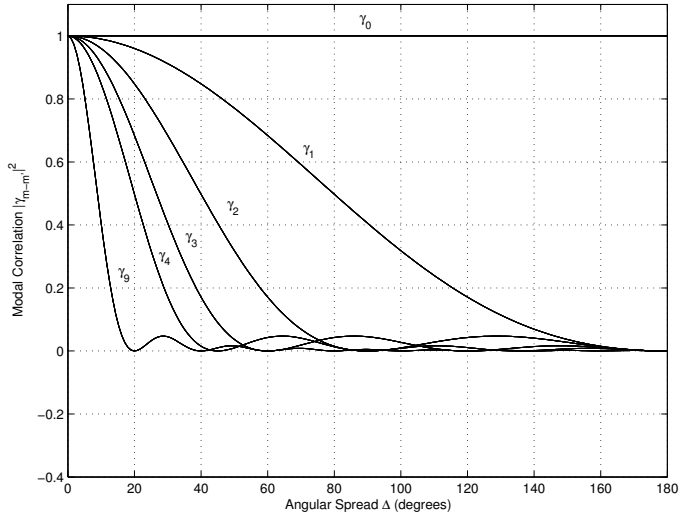

Figure 12-4. Modal correlation versus angular spread Δ of a uniform limited power density surrounding the aperture.

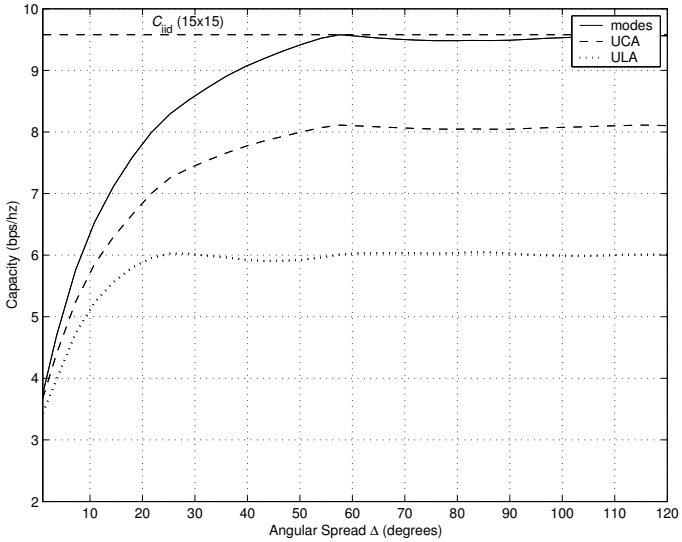

Figure 12-5. Capacity versus angular spread at the transmitter for mode-to-mode communication (modes), uniform linear array (ULA), and uniform circular array (UCA), within spatial regions of radius 0.8λ and isotropic receiver scattering. The mode-to-mode capacity gives the maximum achievable capacity between the two apertures.

fundamental limit to capacity for realistic scattering environments. By characterizing the behavior of possible communication modes for a given aperture, the upper bound on capacity is independent of antenna configurations and array signal processing, and provides a benchmark for future array and space-time coding designs.

In this chapter we have restricted the analysis to 2D circular apertures, however, extension to arbitrary shaped regions can be achieved by using a different choice of orthonormal basis functions (e.g. see [17,19]), however, with the exception of spherical apertures [17], finding analytical solutions for more general volumes poses a much harder problem.

REFERENCES

1. E. Telatar, "Capacity of multi-antenna gaussian channels," Tech. Rep., ATT Bell Labs, 1995.
2. G. J. Foschini and M. J. Gans, "On limits of wireless communications in a fading environment when using multiple antennas," *Wireless Personal Communications*, vol. 6, no. 3, 1998.
3. J.P. Kermoal, P.E. Mogensen, S.H. Jensen, J.B. Anderson, F. Frederiksen, T.B. Sorensen, and K.I. Pedersen, "Experimental investigation of multipath richness for multi-element transmit and receive antenna arrays," in *IEEE Vehicular Technology Conference*, Tokyo, Japan, 2000, pp. 2004–2008.
4. K.I. Pedersen, J.B. Anderson, J.P. Kermoal, and P.E. Mogensen, "A stochastic multiple-input multiple-output radio channel model for evaluation of space-time coding algorithms," in *IEEE Vehicular Technology Conference*, Boston, MA, 2000, pp. 893–897.
5. W. Yu, M. Bengtsson, B. Ottersten, D.P. McNamara, P. Karlsson, and M.A. Beach, "A wideband statisitical model for NLOS indoor wireless MIMO channels," in *IEEE Vehicular Technology Conference (Spring)*, Birmingham, Al, 2002.
6. J.W. Wallace and M.A. Jensen, "Spatial characteristics of the mimo wireless channel: experimental data acquisition and analysis," in *IEEE International Conference on Acoustics, Speech and Signal Processing*, Salt Lake City, Utah, 2001, pp. 2497–2500.
7. G. Athanasiadou, A. Nix, and J. McGeehan, "A microcellular ray-tracing propagation model and evaluation of its narrow-band and wide-band predictions," *IEEE Journal on Selected Areas in Communications*, vol. 18, pp. 322–335, 2000.
8. G. German, Q. Spencer, A. Swindlehurst, and R. Valenzuela, "Wireless indoor channel modeling: statistical agreement of ray tracing simulations and channel sounding measurements," in *IEEE International Conference on Acoustics, Speech, and Signal Processing*, Salt Lake City, UT, 2001, vol. 4, pp. 778–781.
9. Da-Shan Shiu, G.J. Foschini, M.J. Gans, and J.M. Kahn, "Fading correlation and its effect on the capacity of multielement antenna systems," *IEEE Transactions on Communications*, vol. 48, no. 3, pp. 502–513, 2000.

10. D. Gesbert, H. Bolcskei, D. Gore, and A. Paulraj, "Outdoor mimo wireless channels: Models and performance prediction," *IEEE Transactions on Communications*, vol. 50, no. 12, pp. 1926–1934, 2002.
11. J.W. Wallace and M.A. Jensen, "Modeling the indoor MIMO wireless channel," *IEEE Transactions on Antennas and Propagation*, vol. 50, no. 2, pp. 591–599, 2002.
12. A.M. Sayeed, "Deconstructing multi-antenna fading channels," *IEEE Transactions on Signal Processing*, vol. 50, no. 10, pp. 2563–2579, 2002.
13. D. Colton and R. Kress, *Inverse acoustic and elctromagnetic scattering theory*, Springer-Verlag, Berlin, 1992.
14. H.M. Jones, R.A. Kennedy, and T.D. Abhayapala, "On the dimensonality of multipath fields: spatial extent and richness," in *ICASSP 2002*, Florida, 2002.
15. D. Chizhik, G.J. Foschini, M.J. Gans, and J.M. Kahn, "Capacities of multi-antenna transmit and receive antennas: correlation and keyholes," *Electronics Letters*, vol. 36, no. 13, pp. 1099–1100, 2000.
16. F. Demmerle and W. Wiesbeck, "A biconical multibeam antenna for space-division multiple access," *IEEE Transactions on Antennas and Propagation*, vol. 46, no. 6, pp. 782–787, 1998.
17. T.D. Abhayapala, T.S. Pollock, and R.A. Kennedy, "Novel 3D spatial wireless channel model," in *IEEE Vehicular Technology Conference (Fall)*, Orlando, Florida, USA, 2003.
18. T.S. Pollock, T.D. Abhayapala, and R.A. Kennedy, "Introducing space into MIMO capacity calculations," *Journal on Telecommunications Systems*, vol. 24, no. 2-4, pp. 415–436, 2003.
19. D. A. B. Miller, "Spatial channels for communicating with waves between volumes," *Optics Letters*, vol. 23, pp. 1645–1647, 1998.

Acknowledgments

National ICT Australia is funded through the Australian Government's *Backing Australia's Ability initiative*, in part through the Australian Research Council.